Random Vibration Testing Beyond PSD Limitations

Alexander Steinwolf, University of Auckland, New Zealand

The traditional approach to random vibration testing using fast-Fourier-transform simulation has become out-of-date, since it is restricted to consideration of the power spectral density only. The latter means that the FFT approach is based on a Gaussian random signal model. However, the MIL-STD-810F standard establishes that "care must be taken to examine field-measured probability density for non-Gaussian behavior." A test engineer is now required to "ensure that test and analysis hardware and software are appropriate when non-Gaussian distributions are encountered." There is widespread belief that the time waveform replication can address the non-Gaussian issue. However the TWR method is not a simulation, since the replication test is representative of just one road sample measured, not of a road type like the simulation test. This difference between replication and simulation is discussed here. Two methods of non-Gaussian simulation (polynomial function transformation and special phase selection) based on kurtosis and skewness characteristics are considered and examples of simulating various field data are given.

Components, apparatus, and passengers of ground and flight vehicles in steady motion, which constitutes most in-service operations, are subjected to random vibration excitations. This article addresses the issue of simulating such excitations on shakers for product reliability testing purposes. Since digital shaker controllers were introduced, a methodology of converting field data into the frequency domain and using the power spectral density (PSD) function of the vibration under consideration has become a common and well-established approach.

The power spectrum presentation of random data (that is a distribution of vibration energy over the interval of frequencies involved) was implemented first in data analysis, because it gives a clear insight into frequency decomposition of the measured vibration and possible dangerous resonance behavior. Then, the PSD approach was naturally extended to the testing area based on the fact that a vibration time history can be reconstructed from the prescribed PSD by the inverse fast-Fourier transform (IFFT).

The FFT/IFFT procedure has been used by manufacturers of shaker controllers for many years and remained the only tool to realize random excitations on electrodynamic shakers. The technique has numerous advantages and just one restriction. The PSD is a full description of the given random process only if it is stationary and Gaussian. The first condition of being stationary is normally checked and, if not confirmed, the FFT simulation is abandoned. However, if the measured vibration appears do be stationary, no check of the second condition of being Gaussian is ever performed in engineering practice. This is unfortunate.

Quite surprisingly, it is ignored that there might be two different stationary random processes with identical PSDs while their differences are concentrated in other (not PSD) characteristics. When two different time histories with the same power spectrum are converted to the PSD format and then back to the time history domain during shaker simulation, the inputs to the second stage of this conversion will be identical, since the input is the PSD function only. This makes the outputs (i.e., vibration of the shaker table) the same in both cases, while the road data prescribed were different.

In other words, any features of a vibration test specification described by characteristics other than the PSD function will be lost when using the FFT/IFFT simulation technique. How important this observation is can be seen from the following example. Figure 1 shows a time history of automobile body vertical acceleration from road measurements. For these data, the PSD characteristic has been calculated (solid curve in Figure 3), and then a common IFFT simulation procedure was implemented. The resulting time history is plotted in Figure 2, and its PSD is shown by the dotted curve in Figure 3.

Although power spectral density analyses of the road data and the synthetic shaker signal are very close in Figure 3, the time histories presented in Figures 1 and 2 show how erroneous the PSD simulation can be for this example. It is obvious that impacts of these two excitations on vehicle structure, passenger comfort, and reliability of electronic devices will be quite different. This difference between the measured road vibration and the shaker excitation by traditional PSD simulation is due to a specific effect inherent to ground transportation and making this example typical.

When a vehicle is moving over some unusually distinctive irregularity on the road, a high peak , exceeding average level of vibration, occurs in the data record. A pothole is an extreme situation of that kind. But even those roads, which are smooth at first glance, also have rougher sections where the effect manifests itself. When this happens, the time history of vehicle vibration includes high spikes of random intensity. That is what is present in the road data shown in Figure 1, but is absent in the synthetic signal shown in Figure 2.

Although the FFT simulation is a precise reproduction of road data frequency content (see Figure 3), some other characteristics must be involved to fully describe non-Gaussian road data. If we additionally compare the probability density function (PDF) of the road data (solid curves in Figure 4) with the PDF of shaker excitation (dotted curves), the difference between the two signals becomes apparent in both the central PDF section (Figure 4a) and at the tails (Figure 4b), which are shown on a logarithmic scale· The PDF tails are specifically related to the excessive time history peaks from Figure 1 that were not modelled by the PSD simulation that is capable of producing peaks with a height limited to about 4 root-mean-square (RMS) values.

The high peaks in question are sporadic and may seem to be isolated transient events superimposed on a stationary background vibration (see Figure 5). However, if one looks at a long enough record of the same signal like that shown in Figure 6, these high peaks become quite regular, and the assumption of the vibration being stationary remains in place. Therefore, the difference in peak behavior is attributed not to the signal being non-stationary but to the non-Gaussian nature of the stationary vibration data that should be measured properly with sufficient record length.

This issue of simulating realistic time history peaks that are higher than those produced by the FFT/IFFT procedure is just one of the possible non-Gaussian scenarios. There are other cases of non-Gaussian behavior discussed in the literature.

What Standards Say

The problem of going beyond the limits of PSD modelling in shaker testing is not a research matter anymore but a requirement imposed on shaker equipment manufacturers and test labs by the standards. The MIL-STD-810F DOD Test Method Standard[1] establishes that "*care must be taken to examine field measured response probability density for non-Gaussian be-*

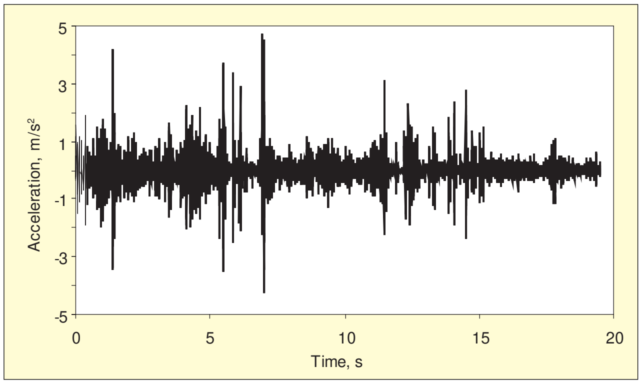

Figure 1. Automobile road data time history.

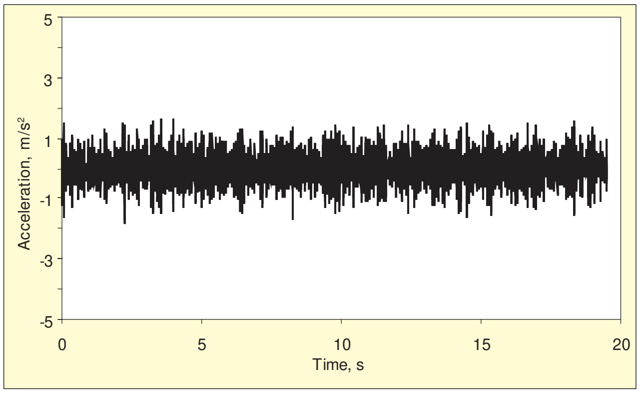

Figure 2. Shaker excitation time history simulated by making use of PSD characteristic only.

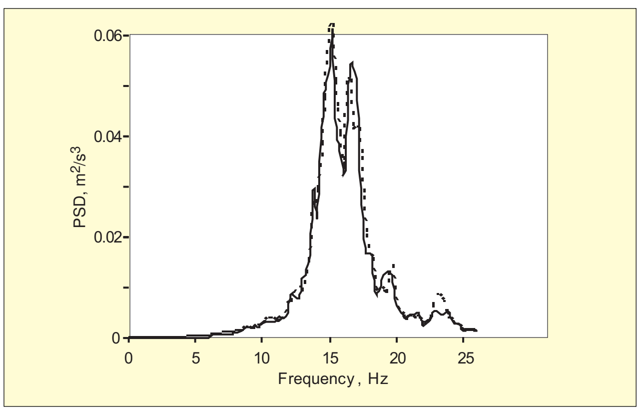

Figure 3. Power spectral densities of the road data (solid curve) and shaker excitation (dotted curve).

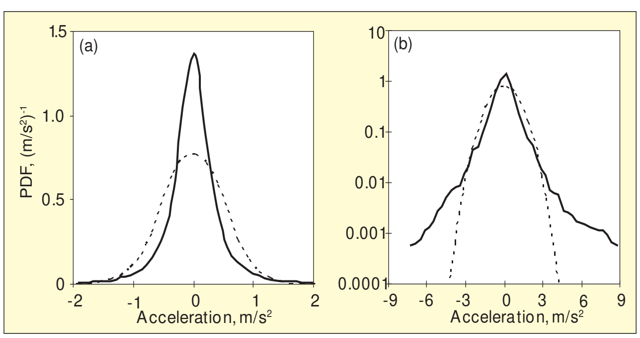

Figure 4. Probability density functions of road data (solid curve) and shaker excitation (dotted curve): a) PDF central section; b) PDF tails.

havior." (page 514.5-11)

Along with this general statement, there is a specific reference to the issue of excessive time history peaks exceeding those generated by FFT simulation: "*in particular, determine the relationship between the measured field response data and the laboratory replicated data relative to three sigma peak*

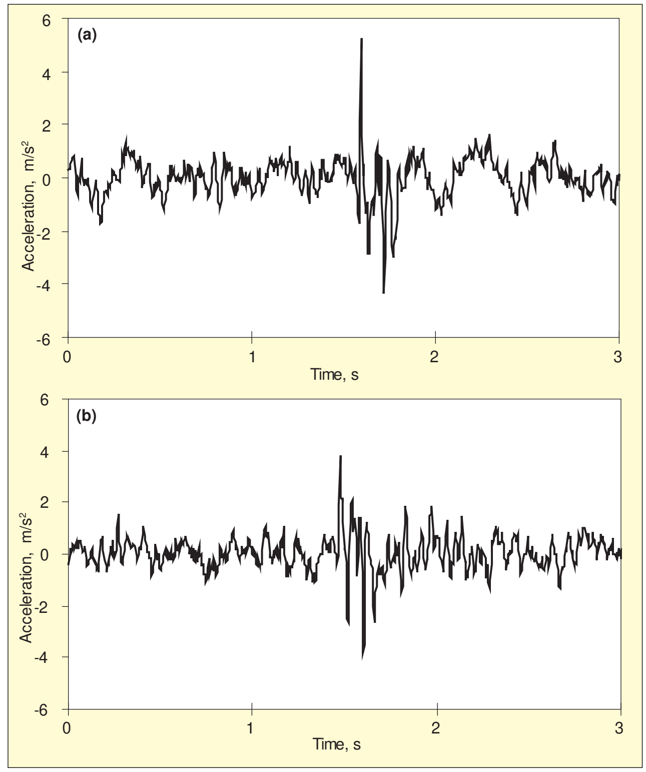

Figure 5. Two 3-second fragments of road data with excessive peaks.

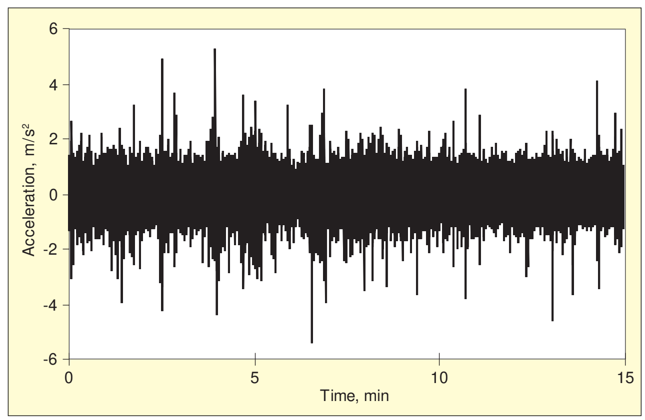

Figure 6. Full time history record of 15 minutes.

height limiting that may be introduced in the laboratory test." (page 514.5-11) In another section, the Standard reads: "*for in-service measured data, the distribution may be non-Gaussian . . . particular care must be given to inherent shaker control system amplitude limiting, e.g., three sigma clipping.*" (page 523.2-13)

The Method 514.5 Vibration of the MIL-STD-810F standard requires test engineers to "*ensure that test and analysis hardware and software are appropriate when non-Gaussian distributions are encountered.*" (page 514.5B-4) A similar requirement is also present in the Method 523.2 Vibro-Acoustic/Temperature of the same standard: "*The test setup should check the test item amplitude distribution to assure that it matches the in-service measured amplitude distribution.*" (page 523.2-13)

The non-Gaussian issue has been also treated seriously in the UK Defence Standard 00-35.[2] Its part 5, Induced Mechanical Environments, establishes that "*Although the vibration experienced by a road vehicle is of random character, it does not usually conform to a Gaussian distribution of amplitudes.*" (page 9) The standard warns that "*the severity of the test . . . may not in general be obtained directly from PSDs because, for tracked and wheeled vehicles, they are unlikely to be an adequate description of the environment.*" (page 113)

Typical PDF tail plots given in the UK Defence Standard 00-35 standard (page 124) are similar to that in Figure 4b and led to the following conclusion: "*the measured data represent a greater damage potential than Gaussian data because of their higher probability of high amplitudes. This nonequivalence can cause difficulties for laboratory testing, because test houses utilize Gaussian random signal generators.*" (pages 9,120)

The latter is repeated several times in more general form in other sections of the UK standard and followed by a statement about the necessity of appropriate shaker simulation methods: "*The non-Gaussian properties are in contrast to the character of vibration generated in test laboratories. Consequently, special steps may need to be taken to avoid undertesting in the laboratory.*" (page 113,129) This echoes a similar declaration in the MIL-STD-810F standard: "*To replicate an autospectral density estimate with a non-Gaussian amplitude distribution, specialized shaker control system software is required.*" (page 523.2-13)

Non-Gaussian Simulation or Waveform Replication?

Specialized shaker control software mentioned above was not available and none of the commercial random vibration controllers had the word "non-Gaussian" in their setup options. Recently the first commercial software capable of kurtosis control was introduced.[3] This product development is based on earlier research efforts[4,5] but, distinct from them, is restricted to just one parameter (kurtosis) and just one of many things that could be achieved with this parameter. Full implementation of non-Gaussian simulation will open much broader horizons. This is yet to come; meanwhile, the time waveform replication (TWR) is frequently referred to as a methodology for non-Gaussian testing.

If a sequence of instantaneous values of the vibration process is reproduced with the help of TWR, then any non-Gaussian features are in place without even considering the PDF. Such a test will be non-Gaussian, however this is ***not a simulation***. The TWR is only a ***replication*** of one particular measured record. Simulation and replication are not synonyms. The ***replication*** test is representative of a given road sample, not of a specified road type. Only the ***simulation*** test can do the latter.

For example, a number of PSD breakpoints are prescribed, and the controller ***simulates*** what did not exist, namely a time history, with as many time history samples as necessary. It is not the same as having a single time history sample and to ***replicate*** it just to have again one sample, but now on the shaker. It is typical that the duration of shaker testing is much longer than the length of available road records. In such a situation, there is no other usage of TWR; i.e., ***replication***, except repetition of the same target profile many times.

In this context, the ***simulation*** approach, like the FFT/IFFT procedure, has an advantage because an unrestricted number of different time history samples can be obtained and joined into a test signal of any length without repetition of the data. It means that a certain variability of test conditions is provided that is lacking in the circle ***replication*** of the same time history record. What we always called "random vibration testing" was the ***simulation*** in terms of the PSD function.

Along with the realistic nonrepetitive shaker excitation, other benefits of the FFT approach are:

- Data storage in PSD format is compact and gives a clear insight into structural resonance phenomena.
- The PSD presentation easily permits averaging of measurements in various conditions and enables a general test specification to be drawn up.
- The test specification can also include components originating not from real road measurements but introduced artificially as a result of previous experience.
- PSD specifications may be obtained not from road data, but from dynamic structural analysis at the design stage.

There is no need to give up all of these benefits by recommending that non-Gaussian data be treated by TWR only. A random vibration controller with non-Gaussian ***simulation*** (not ***replication***!) capabilities is now a reality. Specific non-Gaussian parameters, such as kurtosis and skewness, can be simulated along with PSD modelling. This could meet the requirement of MIL-STD-810F cited at the end of the previous section.

The words "*autospectral density estimate with a non-Gaussian amplitude distribution*" clearly point out to the PSD-plus-PDF simulation approach for random vibration test that had been PSD-only in the past. On the other hand, the MIL-STD-810F standard defines an alternative purpose for TWR: "*Waveform control strategy is not generally applicable to the procedures of Method 514.5 Vibration. It is . . . used for control of transient or short-duration, time-varying random vibration of Method 516.5 Shock.*" (page 514.5-10)

For someone who wants to obey the standards, it should be obvious when we need non-Gaussian ***simulation*** (i.e., PSD-plus-PDF) and when to use time waveform ***replication***. The answer to the question in the heading of this section is, of course, both approaches of going beyond the limitations of the stationary PSD/FFT technique deserve to be further developed, each for its right purpose.

Kurtosis and Crest Factor

As discussed previously, the random vibration data prescribed for shaker simulation should be examined for non-Gaussian behavior. Any deviations from theoretical Gaussian PDF:

$$P_G(x) = \frac{1}{\sigma\sqrt{2\pi}} \exp\left[-\frac{(x-m)^2}{2\sigma^2}\right] \tag{1}$$

must be quantified and included in the test specification in addition to the common PSD requirement.

The principal characters describing non-Gaussian PDF features are skewness λ and kurtosis γ:

$$\lambda = \frac{M_3}{(M_2)^{3/2}} = \frac{M_3}{\sigma^3}, \qquad \gamma = \frac{M_4}{(M_2)^2} = \frac{M_4}{\sigma^4} \tag{2}$$

governed by central moments:

$$M_n = \int_{-\infty}^{\infty} (x-m)^n P(x) dx \tag{3}$$

of the probability density function $P(x)$.

The Gaussian amplitude distribution (Eq. 1) is identified by two parameters: mean value m and variance σ^2, where the latter coincides with the second moment M_2. However, there is no variability in PDF moments higher than the second. For the Gaussian PDF, the skewness and kurtosis related to the third and fourth moments are constants ($\lambda = 0$, $\gamma = 3$). Hence, any other λ and γ values obtained for the prescribed field data would be an indication of Gaussian model failure; i.e., a suggestion about limitations on the use of the PSD/FFT approach for random shaker testing.

Equations 2 and 3 are the theoretical definitions of kurtosis and skewness, whereas for the given time histories, both λ and γ can be calculated via instantaneous values $x(i\Delta t)$ of the digitized data record by time averaging. Estimates for the mean and probability distribution moments are found as follows:

$$m = \frac{1}{N}\sum_{i=1}^{N} x(i\Delta t), \qquad M_n = \frac{1}{N}\sum_{i=1}^{N} [x(i\Delta t) - m]^n \tag{4}$$

and then the kurtosis and skewness are calculated by Eq. 2.

If positive and negative peaks are similar in appearance in the time history (i.e., the PDF is symmetric with respect to the mean value m), then kurtosis is the only additional parameter required to describe deviations from the Gaussian model. On the other hand, if the PDF is asymmetric, then the skewness is nonzero, and its sign will indicate the direction in which the PDF is skewed.

For the purpose of shaker testing, the role of kurtosis is more important, since it is an indicator of the relative height of time history peaks. The latter was characterized before by a crest factor, which is a ratio between the maximum absolute value of the signal and its standard deviation σ:

$$c = \frac{|x(i\Delta t)|_{\max}}{\sigma} \tag{5}$$

The crest factor values are also commonly referred as 2-sigma, 3-sigma, 4-sigma, etc. For more detailed analysis, positive $c^+ = x_{\max}(i\Delta t)/\sigma$ and negative $c^- = x_{\min}(i\Delta t)/\sigma$ crest factor values can be considered separately, resulting from the positive maximum $x_{\max}$ and negative minimum $x_{\min}$, not from one peak with the largest amplitude as in Eq. 5. Any notable difference between c^+ and c^- is a hint about the PDF being skewed (i.e., λ being not zero like the case for a Gaussian signal).

The crest factor is well known; but the kurtosis value is a more robust characteristic, since it summarizes the effect of all excessive peaks, which make the signal non-Gaussian. The crest factor is not so comprehensive and takes into account only one of the peaks – that of the largest amplitude. Furthermore, in contrast to the kurtosis, no strict theoretical value can be defined for the crest factor of a Gaussian process, because the magnitude of the largest peak depends on the length of time history sample even for the same random signal. The theoretical kurtosis value for a stationary Gaussian signal is known and fixed ($\gamma = 3$). As the kurtosis is found by time averaging (see Eq. 4), the longer the data sample the more stable the kurtosis estimate. This is an advantage compared to the traditional crest factor characterization of peak behavior.

For random vibration data with excessive peaks, like the example shown in Figure 1 and discussed previously, the kurtosis value appears to be higher than 3. So if a shaker simulation method could control kurtosis in addition to the PSD and make the shaker excitation kurtosis equal to that observed for the field data, such an advanced non-Gaussian technique would be capable of time-domain peak modelling, but would still be a ***simulation***, not a ***replication***.

A similar approach with the crest factor (Eq. 5) as an additional control parameter is not feasible, since there is no analytical formulation for the relation between the crest factor and FFT amplitudes and phases; neither for Gaussian nor for non-Gaussian signals. Moreover, distinct from the mean, standard deviation, skewness, and kurtosis, the crest factor is not a statistical parameter. It is just one of the time history instantaneous values that are all unpredictable by the definition of random process.

In terms of the probability density function, kurtosis characterizes the sharpness or flatness of the PDF central section and the wideness or narrowness of the PDF tails. A kurtosis value greater than 3 indicates a sharper central section and wider tails (most important) than in the Gaussian PDF with the same standard deviation σ. Widening the PDF tails implies that the probability of high peak occurrence in the time history is larger than that predicted by the Gaussian model. For data samples of finite length (like time blocks in traditional FFT simulation), it means that the signal contains high peaks that would not occur in a Gaussian time history with the same PSD.

While the kurtosis describes the PDF as a function (particularly the tail behavior), the crest factor relates to just one point on the PDF curve – its left or right limit. Crest factor is not a probability of this limiting value but only its position on the argument axis. This is a one more reason to use kurtosis as a peak descriptor for random vibration simulation beyond PSD limitations. Possible ways of how to make a shaker vibration controller be capable of not only sigma limiting (what all commercial controllers can do) but also of sigma stretching are discussed in the next section.

Methods of Non-Gaussian Simulation

Polynomial Function Transformation. The first idea that comes to mind about how to advance from the time signal with a certain PDF (Gaussian) to a signal with a different PDF (non-Gaussian) is to generate a Gaussian time history in a well-known way and then modify it somehow. This can naturally be a functional transformation $y = f(x)$ of the initial time history[6,7,8] where each point of the Gaussian signal in a digitized form $x(i\Delta t)$ is converted into a corresponding instantaneous value of the modified signal $y(i\Delta t)$ that is calculated according to the given function $f(x)$.

The approach is simple but effective as there is an equation:

$$P_2(y) = \frac{P_1(x)}{|f'(x)|} = \frac{P_1(x)}{|dy/dx|} \tag{6}$$

establishing the relationship between the initial $P_1(x)$ and the resultant $P_2(y)$ probability density functions if the transformation function $y = f(x)$ between the signals is given. This transformation should be a monotonically increasing function for Eq. 6 to be valid.

The transformation can be conveniently prescribed in polynomial form:

$$y = f(x) = C_0 + C_1 x + C_2 x^2 + C_3 x^3 \tag{7}$$

that operates not with probability distributions $P_1(x)$ and $P_2(y)$ themselves but with their moment characteristics: standard deviation σ; kurtosis γ; and skewness λ. The third-order polynomial in Eq. 7 is sufficient for skewness and kurtosis manipulations, and the input probability distribution $P_1(x)$ is supposed to be Gaussian in this case.

The methodology under consideration deals with preserving the desired PSD in the first stage of generating Gaussian input and then provides necessary kurtosis and skewness in the second stage of functional transformation $y = f(x)$. Here is the catch: the nonlinear transformation on the second stage affects not only the PDF (that was the objective of the transformation) but also the PSD (that is an unwanted distortion of the frequency domain simulation from the first stage). In some cases this distortion might luckily be nonessential or can be neglected. This is discussed later in more detail.

If the non-Gaussian probability density function (Eq. 6) of the polynomial transformation output $y(t)$ is substituted into Eq. 3 for central moments of the distribution $P_2(y)$, this results in an integral:

$$\begin{aligned} M_n &= \int_{-\infty}^{\infty} (y - m_y)^n P_2(y)dy = \int_{-\infty}^{\infty} \left\{f(x) - m_y\right\}^n P_1(x)\left(\frac{dx}{dy}\right)dy = \\ &\int_{-\infty}^{\infty} \left\{C_0 + C_1 x + C_2 x^2 + C_3 x^3 - m_y\right\}^n \frac{e^{-x^2/2}}{\sqrt{2\pi}} dx \end{aligned} \tag{8}$$

where the standardized Gaussian distribution $P_1(x)$ of the transformation input was taken according to Eq. 1, with the mean $m_x = 0$ and standard deviation $\sigma_x = 1$. The mean value m_y of the transformation output can be found in a similar way and then substituted into Eq. 8.

Integration in Eq. 8 results in the second M_2, third M_3, and fourth M_4 central moments being functions of the three polynomial transformation coefficients C_1, C_2, and C_3. However, after substitution of the moments into Eq. 2 for skewness and kurtosis, the number of independent variables in the polynomial transformation (Eq. 7) reduces to two: $\alpha = C_2/C_1$ and $\beta = C_3/C_1$. These are the two variables the non-Gaussian shaker controller will manipulate in the post-IFFT signal transform:

$$y(t) = C_0 + C_1\left\{x(t) + \alpha x^2(t) + \beta x^3(t)\right\} \tag{9}$$

to achieve necessary skewness λ_y and kurtosis γ_y of the shaker driving signal $y(t)$.

The coefficients C_0 and C_1 in Eq. 9 have nothing to do with the skewness and kurtosis and will be determined after α and β are found from the desired λ_y and γ_y. Coefficient C_0 should be chosen so that the mean value of the non-Gaussian output $y(t)$ is zero or equal to the required DC component (if any) in the driving signal. The role of coefficient C_1 is to ensure that the necessary standard deviation for $y(t)$ is also met; i.e., the voltage level of the driving signal is correct. The last two conditions are common for the controller operation, no mater if the random vibration testing is Gaussian or not.

Expressions for $\lambda_y = Q(\alpha,\beta)$ and $\gamma_y = G(\alpha,\beta)$ as functions of α

and β appear in the form of a ratio of polynomials containing members $\alpha^n\beta^k$ with various powers n and k, from 0 to 6. Thus, there is no analytical solution for α and β for the given λ_y and γ_y. Numerical routines were used to minimize error functions:

$$\varepsilon = \left\{\lambda_y - Q(\alpha,\beta)\right\}^2 + \left\{\gamma_y - G(\alpha,\beta)\right\}^2 \tag{10}$$

or

$$\varepsilon = \left|\lambda_y - Q(\alpha,\beta)\right| + \left|\gamma_y - G(\alpha,\beta)\right| \tag{11}$$

and to find optimal α and β.[7,9,10] If this is the case, the computer code must be one that is capable of doing optimization with constraints to make sure that the constructed transformation function is monotonically increasing.

This approach provides a polynomial transformation with the best precision and can be recommended for generating non-Gaussian time histories off-line. But in a shaker controller loop, the computational time is critical and any numerical solutions in the skewness/kurtosis control algorithm become impractical. There is another way[8] of constructing the Gaussian-to-non-Gaussian transformation function when $f(x)$ is expressed not as a simple polynomial (Eq. 7) but is based on Hermite polynomials and then presented in the form of a truncated Taylor series. This is approximate but gives a closed-form solution:

$$\alpha = \frac{12\lambda_y}{\left(4+\sqrt{6\gamma_y - 14}\right)\left(14-\sqrt{6\gamma_y - 14}\right)} \tag{12}$$

and a similar equation for β. The coefficients α and β then become algebraic functions of skewness λ_y and kurtosis γ_y, which the shaker driving signal must have with current iteration. The latter is a key point in justifying usefulness of the approximate Hermite solution ahead of a 'precise' numerical minimization of functions (Eqs. 10 or 11). An explanation follows.

Simulation of specified skewness and kurtosis values in the shaker excitation can never be achieved in one shot. As in regular FFT/PSD simulation, few iterations are needed to compensate for the influence of the shaker and/or test item dynamics. The approximate equation (Eq. 12) and another one for the second polynomial coefficients β of the Gaussian-to-non-Gaussian transformation (Eq. 9) work well in a shaker controller. Errors in determination of α and β will be corrected in the iterative procedure. This is unavoidable anyway as the degree of kurtosis/skewness transformation by the shaker and test item system is unknown. Experimental results below prove that an approximate solution for α and β is effective.

In many cases, skewness λ_y of the field data PDF is negligible, and the vibration is non-Gaussian in terms of kurtosis only, which now becomes a single target for the polynomial transformation (Eq. 9). For the output signal $y(t)$ to be symmetric, the transformation function $y = f(x)$ should have no members with even powers of x; i.e., the first of the non-Gaussian coefficients α must be zero. This is clearly seen from Eq. 12 – if no skewness; i.e., $\lambda_y = 0$, then $\alpha = 0$. The remaining coefficient β is a function of kurtosis only, and this equation is available to be implemented in the shaker kurtosis controller.

Other, not polynomial, nonlinear transformation functions are possible. One of them was constructed in piecewise form.[7] This solution is actually not for the transformation $y = f(x)$ itself but for its inverse function $x = g(y) = f^{-1}(y)$. The latter adds to the aforementioned issue of difficulties in using numerical routines in a shaker controller, since the transformation function $f(x)$ is then calculated by linear interpolation.[7]

Moreover, the crucial difference between the approach suggested in Reference 7 and this article is that the former is based on and should be used in conjunction with the TWR, while the latter is an alternative to waveform replication and further develops the traditional closed-loop random simulation. Test technicians know which of the two controller operation modes, TWR or random PSD, is easier to set up.

Also, as noted in Reference 7, different Gaussian-to-non-Gaussian time history transformation functions give similar results. Noting their common and inherent tendency of introducing PSD distortions, it is worthwhile to look at another method of non-Gaussian random vibration testing, where nothing is done to the signal after the IFFT generation (i.e., the PSD is not disturbed at all). There is a possibility[4,5,11] of introducing non-Gaussian behavior in the framework of the classic IFFT routine itself, and this is discussed in the next section.

Special Phase Selection. A serious difficulty with the polynomial transformation approach is that any nonlinear function applied to a Gaussian signal changes not only its PDF but the PSD as well. If then the PSD is corrected back to the desired shape by passing the non-Gaussian output signal through a linear filter, this will distort the PDF adjusted initially by the polynomial transformation. Therefore, only by controlling the PSD and PDF independently and simultaneously, not sequentially, the best bi-domain PSD-plus-PDF random simulation can be achieved.

The common and well-established FFT technique of Gaussian random vibration testing is actually to use a multi-frequency signal in the form of Fourier series with a large number of harmonics L:

$$x(t) = \sum_{k=1}^{L} A_k \cos(2\pi k\Delta f t + \phi_k) \tag{13}$$

The amplitudes A_k of the harmonics are determined:

$$A_k = \sqrt{2\Delta f S(k\Delta f)} \tag{14}$$

according to the prescribed PSD shape $S(f)$ and frequency increment Δf. To make the excitation signal (Eq. 13) somewhat of random nature, the phase angles ϕ_k are defined as samples of the random variable uniformly distributed in the range from 0 to 2π.

This model is perfect for digital random vibration controllers, because it allows one to easily correct the input PSD shape according to the feedback acceleration signal collected from the test item. All this convenience and sophisticated modern hardware/software development for the basic iterative procedure of controller operation can be retained when setting up non-Gaussian simulation. Additional control of kurtosis and skewness, responsible for PDF and making the shaker driving signal non-Gaussian, can be achieved without any disturbance to the PSD. The amplitudes A_k are still determined by Eq. 14, and many of the phases ϕ_k are prescribed randomly as before. However, some of the phases are found and fixed in a special way.

Since the number L of frequency components (or frequency lines, as they are called in shaker controller manuals) is large in the generated signal (Eq. 13), there are plenty of random phases ϕ_k which make the time history of the generated non-Gaussian process not unique (see data examples below). Therefore, the special phase selection method, similar to the classic Gaussian technique, can produce any required number of time history blocks without repetition of the same data.

The method has been subjected to comprehensive and thorough computer testing[5] with various PSD profiles reported in the literature for different types of vehicles. Numerical results have shown that all non-Gaussian effects (steepness of the PDF central section, width of the PDF tails, and height of peaks occurring in the time history) can be changed continuously with kurtosis control extended up to very high values of several tens. This worked for different PSD shapes, and precision of PSD fitting remained the same as for ordinary Gaussian techniques.

The latter confirms what was established by the theory of the method.[4] Since the power spectrum of the signal does not depend on phases, any manipulations with them will not change the PSD shape. It means that the non-Gaussian control achieved by these manipulations is performed independently of power spectrum control because variables in the Fourier series model (Eq.13) are separated – amplitudes are responsible for PSD, phase angles for PDF. Thus, the phase selection method meets the aforementioned objective of being a bi-domain (PSD-plus-PDF) random simulation.

Non-Gaussian Simulation Examples

Any non-Gaussian behavior of vibration time histories can

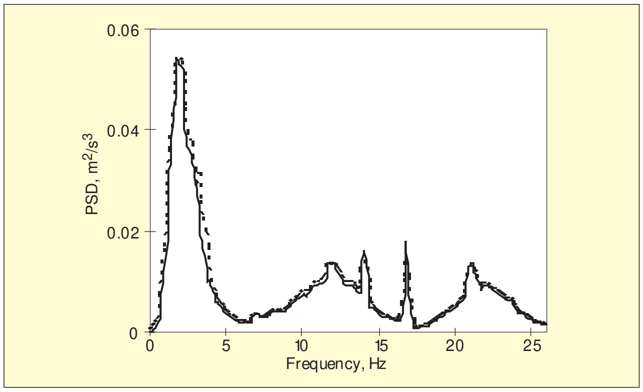

Figure 7. PSDs of road data (solid curve) and shaker excitation (dotted curve).

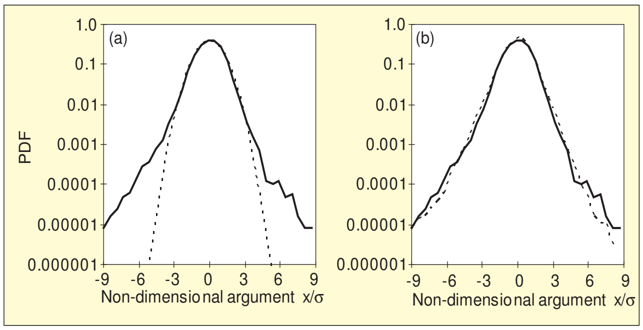

Figure 8. PDFs of road data (solid curves) and shaker excitations (dotted curves): a) Gaussian FFT simulation; b) Non-Gaussian simulation.

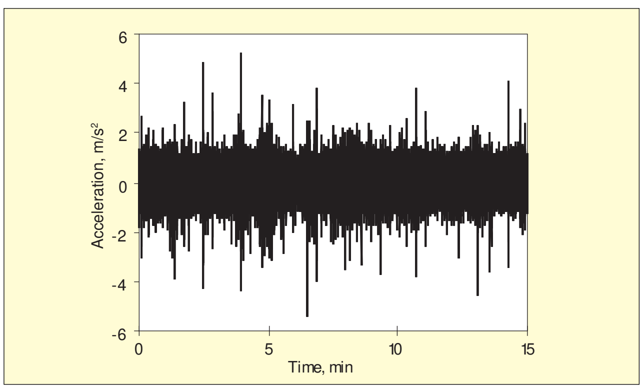

Figure 9. Time history of road data.

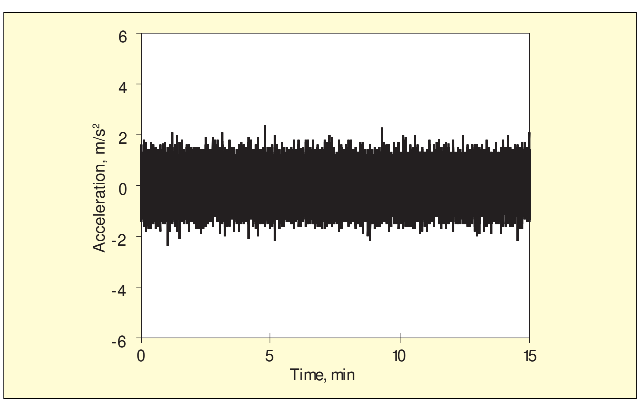

Figure 10. Gaussian FFT simulation time history.

be simulated by the above methods. In the shaker testing area, a case of higher than Gaussian probability at the PDF tails is of special interest. As discussed previously, an increase in the kurtosis of vehicle vibration indicates the occurrence of unusually high peaks in the data set. The Gaussian model covers peaks up to some 4 RMS values (4σ values). However, peaks higher than that have been found to be typical of vibration

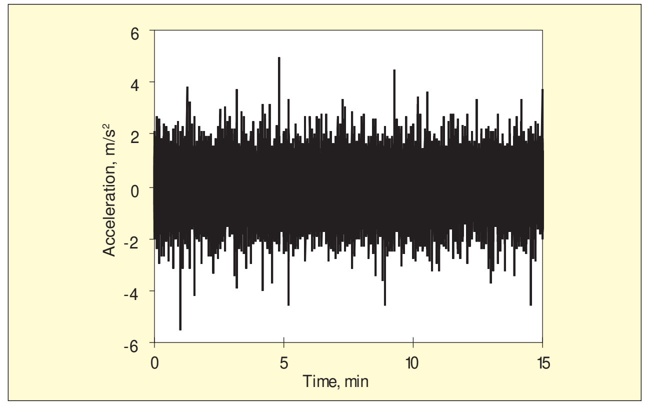

Figure 11. Non-Gaussian simulation time history

records measured in trucks and military trailers,[12,13] automobiles,[5,14] and aircraft.[15]

Polynomial Function Transformation. The first example of non-Gaussian vibration simulation is an illustration of the polynomial transformation method. The road data record to be simulated was automobile vertical vibration acceleration measured on the body floor when driving on a highway at 130 km/hour. The recording was much longer than those normally taken for regular PSD analysis. With a sampling rate of 256 Hz, the time history record was about 15 minutes long, resulting in N = 230,000 data points. This is the price to pay for being able to simulate realistic kurtosis and crest factor values observed in road data. It should be taken into account that the higher the time history peak, the less frequently it occurs. Therefore, longer data records are necessary to have representative statistical material about the high peaks and to calculate the experimental PDF tails properly.

The PSD and PDF obtained for the road data under consideration are depicted by solid curves in Figures 7 and 8. Note widening of the PDF tails compared to those of the regular Gaussian shaker excitation whose PDF is shown in Figure 8a by the dotted curve. The road data kurtosis value was $\gamma = 4.7$ (notably larger than $\gamma = 3$ for a Gaussian signal) and the crest factor $c = 10.2$ was more than twice the Gaussian value for such a record length. The skewness value was mild ($\lambda = -0.18$).

Initially, the traditional FFT simulation procedure for commercial random controllers was implemented and the shaker excitation PSD, shown by the dotted curve in Figure 7, appeared to be very close to the road data PSD. But similar to what was discussed previously, there were no realistic excessive peaks in the Gaussian shaker vibration time history (compare Figures 9 and 10) and the PDF tails for the road and shaker data were different (see Figure 8a).

Then, the FFT-generated time histories with the fitted PSD were subjected to polynomial transformation (Eq. 9) with the coefficient α found by Eq. 12 and the coefficient β by a similar equation providing the desired kurtosis and skewness values. Since the non-Gaussian time histories obtained in this way had somewhat lower crest factors and generally less severe peaks, further increase of the shaker excitation kurtosis was required.

The final result of the non-Gaussian simulation is shown in Figure 11. Comparison of this time history with the road record in Figure 9 and with what can be achieved by the Gaussian FFT procedure (Figure 10) leads to an obvious conclusion. Also, the shaker excitation PDF (dotted curve in Figure 8b) is now very close to the road data PDF in contrast to the probability distribution results of the traditional Gaussian technique in Figure 8a. The most important accomplishment is that the shaker excitation is similar to the road record, but not a replication of it. Any number of different time history data samples, all equally close to the road time history (see Figure 12), can be obtained by the same polynomial transformation applied to common Gaussian time blocks generated by a conventional random vibration controller for the given PSD.

Special Phase Selection. The next example is also for auto-

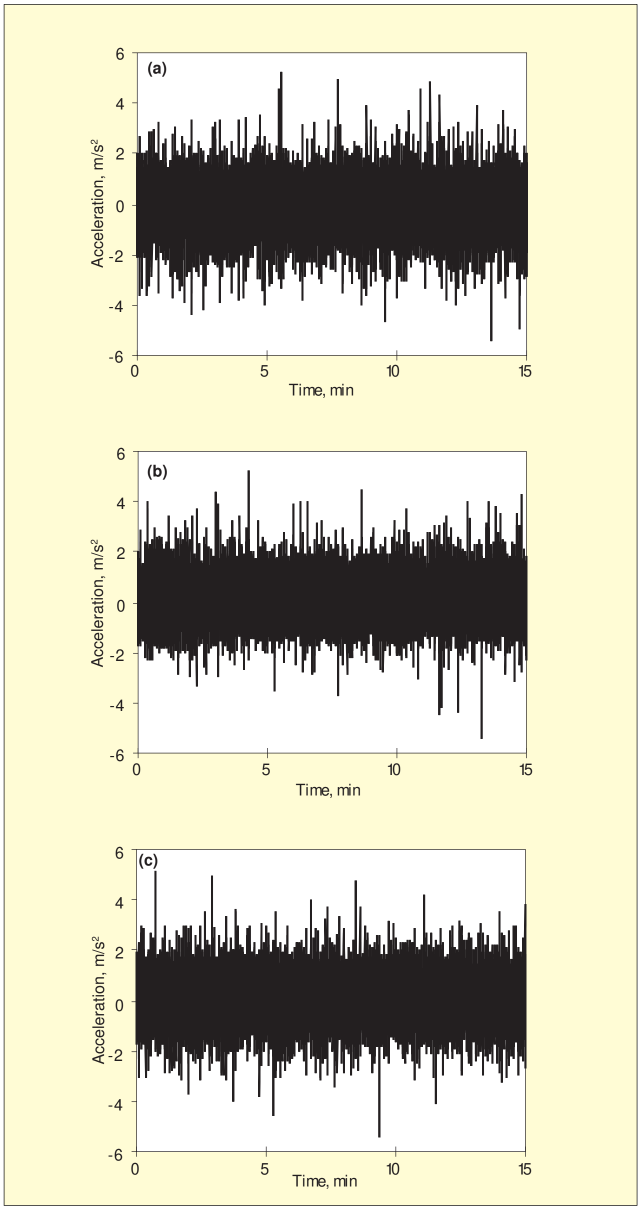

Figure 12. Different time history samples obtained for non-Gaussian simulation by the polynomial transformation.

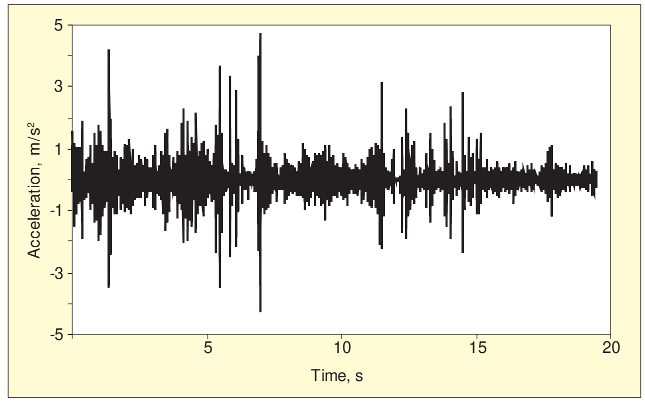

Figure 13. Time history of road data.

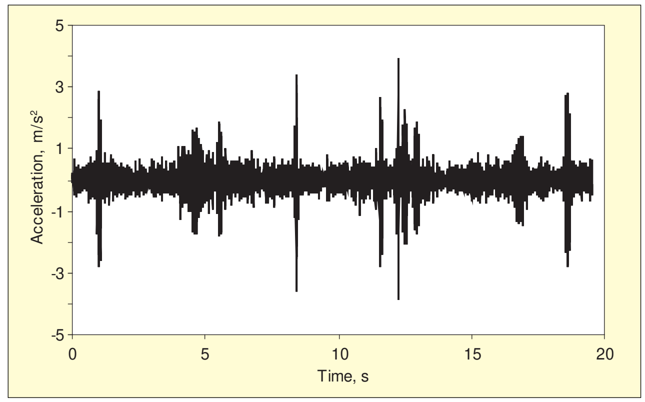

Figure 14. Non-Gaussian simulation with special phase selection.

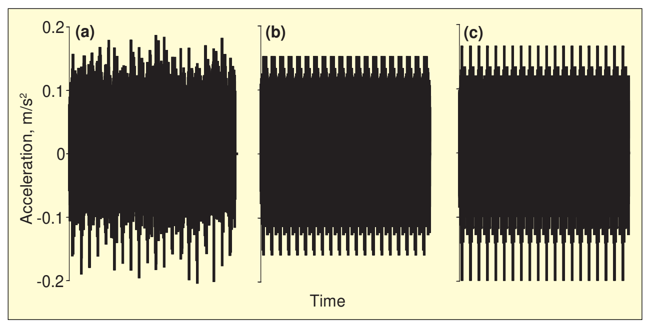

Figure 15. Time histories: a) road data encompassing 20 test runs; b) TWR testing if softest road run is used; c) TWR testing if most severe road run is used.

mobile vibration simulation, particularly that shown in Figure 1 and discussed earlier. The road was rougher than in the previous example, so the peaks in the time history were more severe compared to the Gaussian shaker excitation (Figure 2), which can be generated by a commercial random vibration controller in terms of PSD. For this example the phase selection method was implemented. Figures 13 and 14 illustrate the closeness of the non-Gaussian shaker excitation time history to the road data record, contrary to what is seen in Figures 1 and 2. The phase method can be set up to model not only kurtosis but also skewness and this was demonstrated in Reference 16.

Comparison with Time Waveform Replication. The results in the previous two sections show that simulation of non-Gaussian high peaks in a vibration time history can be achieved by kurtosis control with the help of the methods discussed. If the TWR is used for the same purpose, the difference is that with the replication of the field record, nothing else except this particular record can be seen on the shaker. However, this record will never be exactly repeated if the vehicle is driven again over the same road section, not to mention another section of road of even the same type.

Such a situation is shown in Figure 15a, where 20 data records obtained in 20 runs over the same road section are joined together. These runs were supposed to be identical, but actually this is not the case. The combined time history demonstrates clearly that there is an inherent variability that is lost if we utilize a common TWR practice – when someone has a field record but needs a test 20-times longer, he simply plays the record 20 times and gets what is shown in Figures 15b and 15c.

If the record captured on the road is something intermediate compared to the other 19 records that actually exist but were not measured, then this results only in the loss of variability. However, the worst happens if the field record used in the TWR was actually the softest (Figure 15b) or the most severe (Figure 15c) ride. These will be the cases of under- or over-testing with unpleasant consequences for the test engineer.

Traditional random testing by FFT simulation certainly provides variability. But if the original field data is different from Gaussian, like the example under consideration, then the benefit of having variability is definitely not a sufficient compensation for differences in the behavior of time history peaks in Figures 16a and 16b (both in peak height and asymmetry). The answer to the problem is non-Gaussian simulation. A combination of the special phase selection method and polynomial transformation was used to produce the 20-times longer non-

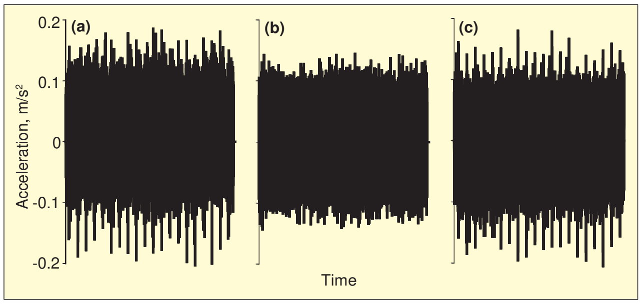

Figure 16. Time histories: a) road data encompassing 20 test runs; b) Gaussian FFT simulation; c) non-Gaussian shaker simulation.

Gaussian simulated time history depicted in Figure 16c.

First the phase selection was implemented to achieve quasi-periodicity of run repetitions seen in the original combined record in Figure 16a. Then the polynomial transformation added necessary skewness to make negative peaks higher then positive like in the road record. As a result, high peaks absent in the FFT simulation are now present in the shaker vibration. Their height, which would be constant with the TWR, varies realistically from frame to frame. This can be continued for any number of time frames with each representing another road run.

Experimental Results

The non-Gaussian numerical simulation examples shown in the previous section demonstrate how a time history with a specified PSD, kurtosis, and skewness can be generated. It remains to decide what this time history is supposed to be: the driving signal or the output feedback signal from an accelerometer. If it's the latter (as in Reference 7), then, after converting the non-Gaussian kurtosis/skewness behavior into the time domain, there is no other way of actually reproducing it on the shaker except TWR.

But what if we do not hurry with converting the specified kurtosis value into a non-Gaussian acceleration time history, but first control and adjust the kurtosis for the driving signal so that the output kurtosis is equal to the specified value. This is exactly what a commercial random FFT controller is doing with the PSD, because the input and output PSDs are different due to system dynamics. The same occurs with kurtosis. It changes for the acceleration feedback signal compared to that of the driving signal, as does the skewness.

There is no need in TWR to experimentally implement the non-Gaussian methods of polynomial transformation or special phase selection. Kurtosis and skewness of the shaker driving signal can be considered and included in the iteration procedure simultaneously with the PSD. This has already been realized successfully with the phase selection method.[5] Now the polynomial transformation method is used as well and the results are reported below.

An approximation for α (Eq. 12) and another equation for the second coefficient β of the polynomial transformation (Eq. 9) were used rather than a numerical minimization of Eqs. 10 or 11 for reasons discussed earlier. Any use of numerical routines to exercise a kurtosis iteration would inevitably slow down the controller operation. Actually there is no need to refine the approximate values for the driving signal kurtosis. The iterative procedure was able to compensate for any kurtosis errors in the driving signal by increasing or decreasing the target kurtosis value for the next iteration.

No Resonances of Shaker Armature and Test Item. Before looking at non-Gaussian behavior, we need to check how kurtosis addition affects a traditional PSD simulation. Figure 17 shows that the PSD iterations look familiar with the acceleration feedback PSD gradually approaching the triangle target profile depicted by the dotted curve (exactly like the one for no kurtosis). These experimental results are for where kurtosis $\gamma = 6$, but the same frequency domain precision was observed in two other experiments where $\gamma = 9$ and $\gamma = 3$ (the

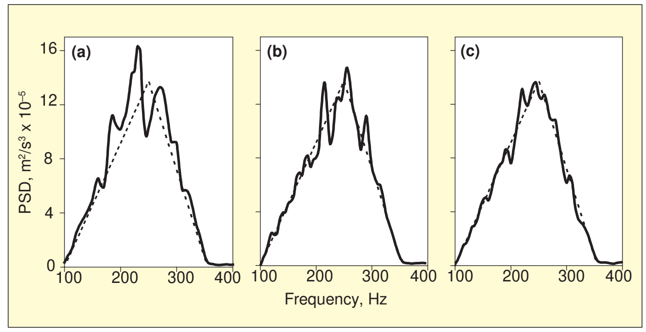

Figure 17. PSDs of acceleration feedback for non-Gaussian shaker simulation with kurtosis γ=6: a) second iteration; b) third iteration; c) fifth iteration.

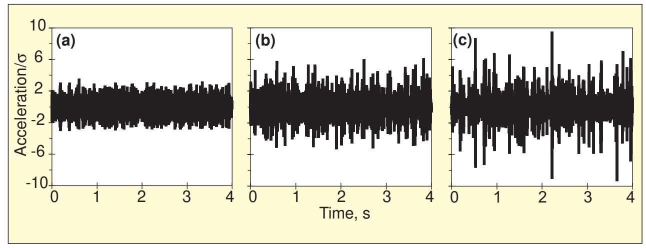

Figure 18. Time histories of acceleration feedback signal for non-Gaussian simulation by the polynomial transformation method: a) Kurtosis γ=3; b) Kurtosis γ=6; c) Kurtosis γ=9.

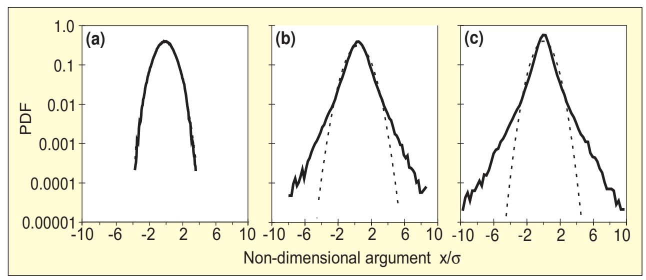

Figure 19. PDFs of acceleration feedback signal (solid curve) for non-Gaussian shaker simulation by the polynomial transformation method (theoretical Gaussian PDF is shown by dotted curve: a) Kurtosis γ=3; b) Kurtosis γ=6; c) Kurtosis γ=9.

Gaussian case). However there were dramatic differences between all three experiments when the time domain and the probability distribution domain results are examined.

It took two iterations for the kurtosis to stabilize. Depending on the target kurtosis value (3, 6, or 9), the time histories of the acceleration feedback (Figure 18) demonstrate different peak behavior with crest factors of c = 3.6, c = 7.5, and c = 9.8, respectively. To emphasize differences in crest factor, the vertical axis is non-dimensional to represent the ratio between actual acceleration values and the overall standard deviation in m/s^2 for the entire time history record.

It might be hard to believe but all three time histories shown in Figure 18 have the same standard deviation and are characterized by the same PSD. These time history plots show the difference between the Gaussian and non-Gaussian random vibrations that was always overlooked. In terms of probability distributions, particularly with PDFs depicted on the logarithmic vertical scale (see Figure 19), the difference between probabilities of certain σ levels can be seen.

In the Gaussian experiment, the probability of 0.0003 corresponds to 3.6σ time history values (Figure 19a) and these σ amplitudes cannot be set for higher probability of occurrence with the help of a Gaussian controller. Using a non-Gaussian random controller, a test engineer would be able to raise this probability 14 times by prescribing a kurtosis of 6. When doing so, the probability of 0.0003 will correspond now to 5.6σ values (Figure 19b). If the kurtosis value is further increased from γ = 6 to γ = 9 (Figure 19c), the probability of 5.6σ time history values also increases 2.5 times more than for kurtosis

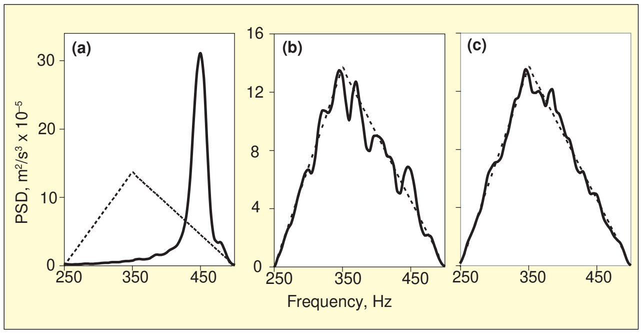

Figure 20. Gaussian simulation for a test item with a resonance; PSDs of acceleration feedback (solid curve) and triangle target PSD profile (dotted curve): a) first iteration; b) second iteration; c) third iteration.

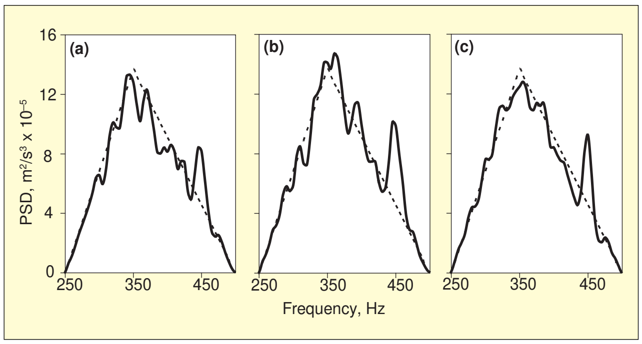

Figure 21. Non-Gaussian simulation (kurtosis γ=6) by the polynomial transformation method; PSDs of acceleration feedback with an unwanted resonance of the test item at 450 Hz: a) second iteration; b) fourth iteration; c) sixth iteration.

$\gamma = 6$ and so on. The horizontal axes in Figures 19 are non-dimensional after dividing real acceleration values by the standard deviation σ. Note in Figure 19 that with the kurtosis increase, the PDF tails become not only wider but also longer.

Resonance of Test Item in the Excitation Frequency Interval. The non-Gaussian method of polynomial transformation worked well, but this was with no resonances of the shaker/(test item)/fixture system in the frequency interval of the specified PSD profile. When the same triangle profile was shifted by 150 Hz to higher frequencies, it covered a resonance at about 450 Hz. This is seen in Figure 20a showing the PSD of the acceleration feedback on the first iteration made with the uniform PSD of the driving signal. This resonance was quickly reduced when the Gaussian PSD control was used (Figures 20b and 20c).

Starting from the third iteration of the Gaussian experiment, the feedback PSD shape was perfect (Figure 20c). However, this was not the case when a non-Gaussian test specification with kurtosis $\gamma = 6$ and the same PSD profile was tried. The resonance at the right slope of the profile remained at an unacceptable level no matter how many iterations were carried out (Figures 21). The controller was trying to reduce this resonance and this can be seen from the driving signal PSDs (Figures 22).

The excitation PSD level at the resonance frequency (thin curve in Figures 22 a,b,c) was further decreased on each next iteration of FFT control in response to the feedback peaks higher than the PSD profile value at 450 Hz (see Figure 21). Why the resonance peak stayed is clear from the thick curve in Figures 22 a,b,c that is the PSD of the non-Gaussian driving signal obtained by the polynomial transformation method. Because of nonlinear distortions, the PSD of an IFFT-generated input acquires uncontrollable noise that is much larger (see thick curves) than the value prescribed by the controller feedback loop (thin curves). Note that the polynomial transformation output (thick curve) remains the same on all iterations (second, then fourth, then six), not reacting to the controller making the target input PSD smaller and smaller.

The aforementioned behavior at the resonance is typical for the polynomial (or any other) nonlinear transformation method

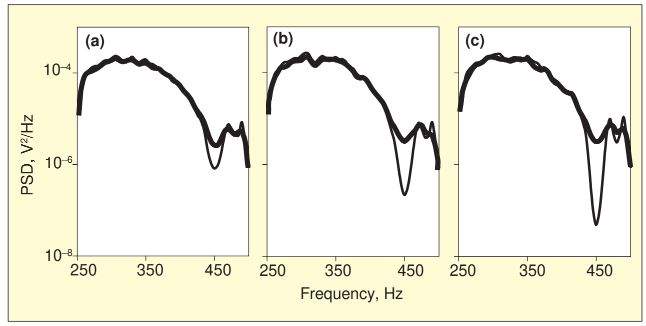

Figure 22. Non-Gaussian simulation (kurtosis γ=6); PSDs of the driving signal before (thin curve) and after (thick curve) polynomial transformation: a) second iteration; b) fourth iteration; c) sixth iteration.

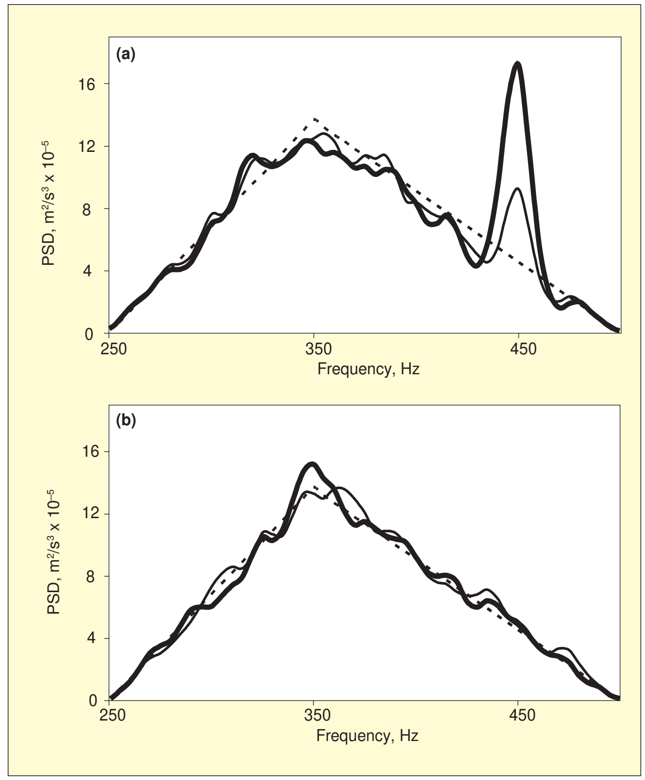

Figure 23. Acceleration PSDs with a resonance of the test item (kurtosis γ=6 – thin curve, kurtosis γ=9 – thick curve, and triangle target PSD profile – dotted line): a) polynomial transformation method; b) special phase selection method.

and restricts its use to no resonance cases or very mild kurtosis values. When the target kurtosis value was raised from $\gamma = 6$ to $\gamma = 9$, the height of the uncontrollable resonance peak increased dramatically (see Figure 23a). This is because more PSD distortions resulted from further increase of the PSD noise level present in the shaker driving signal near the resonance frequency. Nothing like this happens with the special phase selection method.

Regardless of the target kurtosis value, the special phase selection method, when implemented in the same experiment with resonance, provided a perfect fit of the acceleration feedback PSD (Figure 23b). Note that, with the polynomial transformation method, some extra kurtosis value was always needed for the drive signal (thin curves with square points in Figures 24a and b), and it took three iterations to achieve the target kurtosis value for the acceleration feedback (thick curves with circle points). For the phase selection method (Figure 24c), the kurtosis of the drive and feedback are close, and the target value is actually achieved on the first iteration. A Gaussian simulation with the same PSD is shown in Figure 24 as a zero iteration for comparison.

Conclusions from Experiments. Based on the results of the experiments discussed, it can be concluded that the polyno-

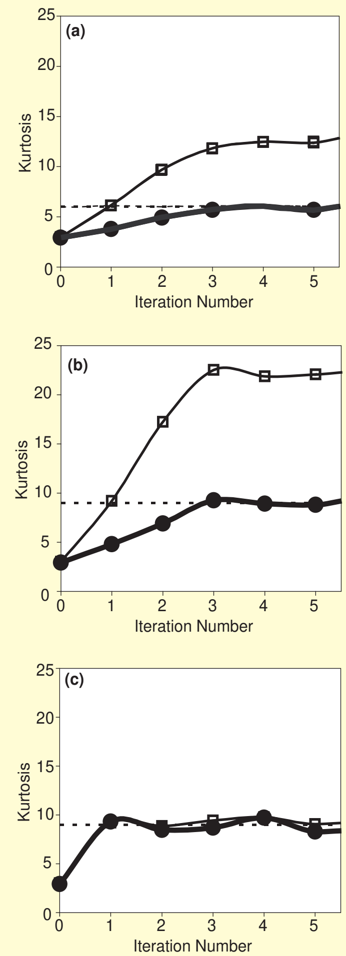

Figure 24. Kurtosis control process (drive signal kurtosis – thin curve, acceleration feedback kurtosis – thick curve, target kurtosis – dotted line): a) polynomial transformation for target kurtosis γ=6; b) polynomial transformation for target kurtosis γ=9; c) special phase selection method for kurtosis γ=9.

mial (or any other nonlinear) transformation method is easier to use. For mild non-Gaussian deviations, it is quite useful, because PSD distortions are not essential and simplicity becomes the main consideration. However difficulties arise not only with stronger non-Gaussian requirements in the test specification, but also if any resonances of the test object or the shaker armature are present in the excitation frequency band.

The polynomial method manages resonances badly. It cannot achieve low enough PSD levels for the driving signal at resonance frequencies, because the polynomial transformation of harmonic components causes nonlinear distortions at all frequencies. There is no such difficulty with the special phase selection method, since the parameters used for kurtosis control (the phases) have no effect on the PSD and the frequency domain specification is not affected by additional non-Gaussian simulation.

References

1. MIL-STD-810F, *Department of Defense Test Method Standard for Environmental Engineering Considerations and Laboratory Tests*, USA, January 2000.
2. Defence Standard 00-35, *Environmental Handbook for Defence Materiel, Part 5: Induced Mechanical Environments*, UK Ministry of Defence, May 1999.
3. Van Baren, P., “The Missing Knob on Your Random Vibration Controller,” *Sound and Vibration*, Vol. 39, No 10, pp. 2-7, 2005.
4. Steinwolf, A., “Approximation and Simulation of Probability Distributions with a Variable Kurtosis Value,” *Computational Statistics and Data Analysis,* Vol. 21, pp. 163-180, 1996.
5. Steinwolf, A., “Shaker Simulation of Random Vibrations with a High Kurtosis Value,” *Journal of the Institute of Environmental Sciences,* Vol. XL, No 3, p. 33-43, May/June, 1997.
6. Merritt, R. G., “A Stochastic Model for the Pulse Method – Part 2: Random Part,” *Proceedings of the 43rd IEST Annual Technical Meeting*, Los Angeles, CA, pp. 121-129, 1997.
7. Smallwood, D. O., “Generating Non-Gaussian Vibration for Testing Purposes,” *Sound and Vibration,* Vol. 39, No 10, pp. 18-24, 2005.
8. Winterstein, S. R., “Nonlinear Vibration Models for Extremes and Fatigue,” *ASCE Journal of Engineering Mechanics*, Vol. 114, pp. 1772-1790, 1988.
9. Winterstein, S. R., and Lange, C. H., “Moment-Based Probability Models for Wind Engineering Applications,” *Proceedings of the 10th ASCE Engineering Mechanics Specialty Conference*, Boulder, CO, Vol. 1, pp. 159-163, 1995.
10. Gurley, K. R., and Kareem, A., “Analysis Interpretation Modelling and Simulation of Unsteady Wind and Pressure Data,” *Journal of Wind Engineering and Industrial Aerodynamics*, Vol. 69-71, pp. 657-669, 1997.
11. Steinwolf, A., “Shaker Dynamic Test for Vehicle Random Vibrations with Asymmetrical Probability Distribution,” *Proceedings of the 26th Int. Symposium on Automotive Technology and Automation (Dedicated Conference on Mechatronics)*, pp. 711-718, Aachen, Germany,1993.
12. Connon, W. H., “Comments on Kurtosis of Military Vehicle Vibration Data,” *Journal of the Institute of Environmental Sciences*, No 6, pp. 38-41, September/October 1991.
13. Charles, D., “Derivation of Environment Descriptions and Test Severities from Measured Road Transportation Data,” *Environmental Engineering*, December 1992, pp. 30-32; March 1993, pp. 25-26.
14. Steinwolf, A., “Analysis and Approximation of Probability Distribution of Vehicle Random Vibrations with Consideration of Kurtosis and Skewness Values,” *Proceedings of 5th Int. Conference on Recent Advances in Structural Dynamics,* Vol. 2, pp. 785-794, Southampton, England, 1994.
15. Wolfe, H. F., Camden, M. P., and Brown, D. L., *et al.*, “Six Sigma Effects on the Response of a Cantilevered Beam with Random Excitation,” *Proceedings of the 67th Shock and Vibration Symposium*,” pp. 499-508, Monterey, CA, 1996.
16. Steinwolf, A. and Ibrahim, R. A., “Analysis and Simulation of Asymmetric Probability Distributions During Fundamental and Environmental Random Vibration Tests,” *Proceedings of the 43rd IEST Annual Technical Meeting,* pp. 48-55, Los Angeles, CA, 1997.

The author may be reached at: a.steinwolf@auckland.ac.nz.